Seismic Risk Management of Existing Reinforced Concrete Buildings in the Cascadia Subduction Zone

Katsuichiro Goda[1] and Solomon Tesfamariam, M.ASCE[2]

Abstract: Through evolution of building design codes in active seismic regions, life safety performance limit state has been met. Unacceptably high economic loss during the 1994 Northridge and 1995 Kobe earthquakes, however, has brought forward a new design paradigm: performance-based earthquake engineering (PBEE). In this study, the PBEE is extended to study: (1) effect of three earthquake types, namely shallow crustal earthquakes, deep in-slab earthquakes, and megathrust Cascadia interface earthquakes, on loss assessment; (2) consideration of main shock–aftershock (MS-AS) sequences as earthquake excitation; and (3) multivariate seismic demand modeling for multicriteria seismic performance evaluation. This is applied to a 4-story nonductile reinforced concrete (RC) frame located in Victoria, British Columbia (BC), Canada. Through this case study, it is highlighted that the sources of ground motion have significant effects on loss assessment. Furthermore, influences of MS-AS earthquake sequences and multivariate seismic demand models on the expected seismic loss ratios are in the order of 10%. In light of this, for any future seismic risk management, it is proposed to have an evolutionary assessment framework that is adaptive to the current state of scientific knowledge and evidence. **DOI: 10.1061/(ASCE)NH.1527-6996.0000206.**

Author keywords: Earthquake engineering; Decision making; Risk management.

Introduction

Building sustainable and resilient communities against large earthquakes is a global problem in active seismic regions. A catastrophic earthquake and its cascading events, such as tsunami, jeopardize the integrity and normal functioning of buildings and urban infrastructure. Incurred seismic damage includes loss of life and limb, direct financial loss to properties and lifeline facilities, and indirect loss attributable to the compounding effects of the direct loss across regional and national economies. Learning from damaging earthquakes in the past, seismic design provisions of modern building codes have evolved continuously (i.e., increase of design base shear and implementation of ductile beam-column joints; e.g., Mitchell et al. 2010), achieving the improved life safety objectives. A historical overview of earthquake impact is presented in Fig. 1, which shows monetary loss and fatalities attributable to previous earthquakes (occurred between 1980 and 2011) for different geographical regions. The figure highlights that earthquakes in the United States, New Zealand, and Japan have caused considerable monetary loss, while the fatalities are minimal (except for the 1995 Kobe earthquake and the 2011 Tohoku earthquake). In contrast, the loss of lives in the South American and Asian earthquakes is considerably high. This indeed corroborates the enhanced life safety performance of the modern seismic design codes. It also provides the motivation for a performance-based earthquake engineering (PBEE) methodology (Cornell et al. 2002; Wen and Ellingwood 2005; Goulet et al. 2007; Jayaram et al. 2012), which aims at reducing the economic and financial consequences of earthquake disasters, in addition to the life safety requirement.

An accurate assessment of potential impact of future destructive earthquakes is essential for effective disaster risk reduction. The PBEE methodology has been developed to assess seismic vulnerability of structures that contributes to specified levels of consequences by taking into account key uncertainty and dependency of the risk assessment (Cornell et al. 2002; Goulet et al. 2007). Recently, further sophistication and innovation have been achieved in the PBEE. One of the major aspects is extension to subduction earthquakes (e.g., Japan, Taiwan, and Indonesia) by taking into account different physical environments for earthquake occurrence and ground motion propagation, in comparison with those in the active continental crust (e.g., California and Europe). The ground motion caused by large subduction earthquakes have greater seismic demand potential for flexible buildings that are susceptible to long-period and long-duration excitations (Goda and Hong 2006; Koduru and Haukaas 2010; Takewaki et al. 2011; Raghunandan et al. 2015). For vulnerability assessment of structures, seismic demand prediction models need to be developed using large subduction earthquake records, such as those from the 2011 moment magnitude scale (M_w) 9 Tohoku earthquake. Incorporating aftershock ground motion into the PBEE procedure, which primarily concerns main shock ground motion, is a timely research topic. As repairs of main shock−damaged buildings are not usually completed during an ongoing aftershock sequence, large aftershocks potentially increase the damage severity of main shock–damaged buildings and cause additional loss (Li and Ellingwood 2007; Ruiz-Garcia 2012; Tesfamariam et al. 2015). Moreover, damage assessment and loss estimation components of the PBEE procedure have been extended to consider different types of seismic loss generation mechanisms (e.g., noncollapse, collapse, and demolition) based on multiple engineering demand parameters, such as maximum and residual interstory drift ratios and peak floor acceleration (Ramirez and Miranda 2009; Jayaram et al. 2012). These

[1]Senior Lecturer, Dept. of Civil Engineering, Univ. of Bristol, Queen's Bldg., University Walk, Bristol BS8 1TR, U.K. (corresponding author). E-mail: Katsu.Goda@bristol.ac.uk

[2]Associate Professor, School of Engineering, Univ. of British Columbia, Okanagan Campus, 3333 University Way, Kelowna, BC, Canada V1V 1V7. E-mail: Solomon.Tesfamariam@ubc.ca

Note. This manuscript was submitted on February 10, 2015; approved on September 14, 2015; published online on December 18, 2015. Discussion period open until May 18, 2016; separate discussions must be submitted for individual papers. This paper is part of the ***Natural Hazards Review***, © ASCE, ISSN 1527-6988.

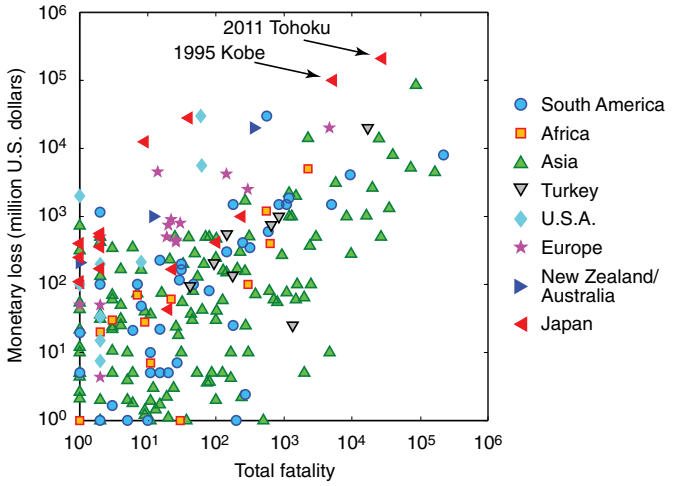

Fig. 1. Total fatality versus monetary loss for worldwide earthquakes in 1980–2011

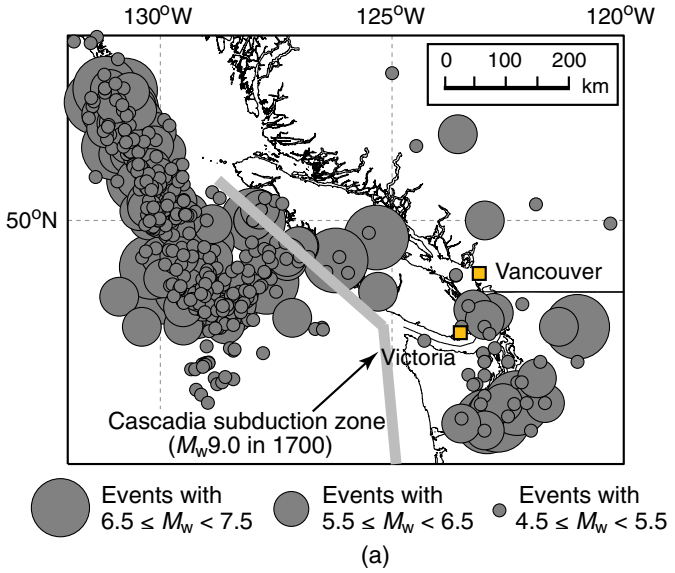

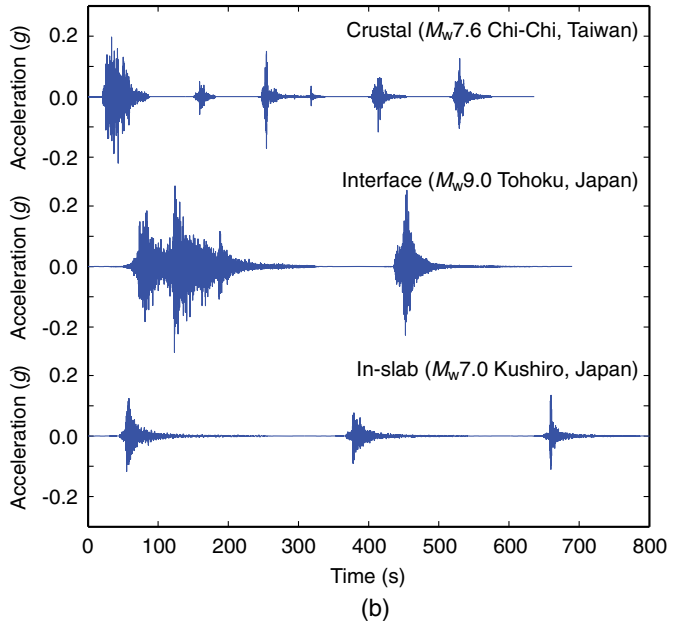

Fig. 2. (a) Regional seismicity in southwestern British Columbia, Canada; (b) sample ground motion records for shallow crustal, megathrust interface, and deep in-slab events

improvements promote new opportunities to develop more effective policies and strategies for earthquake risk mitigation at local, regional, and national scales.

Victoria, the capital city of province of British Columbia (BC), Canada, on Vancouver Island, is focused upon as a case study to illustrate the proposed PBEE method. In Victoria, seismic vulnerability of existing buildings is a major concern because of the use of older design codes and/or poor construction practices at the time of design and construction. A previous regional seismic risk assessment study carried out by Onur et al. (2005) indicated that seismic risk to vulnerable parts of older constructions in Victoria is high. In addition, a recent study by AIR Worldwide (2013) suggested that regional economic loss associated with a hypothetical M_w9 Cascadia earthquake scenario can be significant. Most of these old buildings are required to be further assessed and upgraded to mitigate potential economic consequences attributable to seismic damage.

Victoria is situated in an active seismic region, affected by complex regional seismicity (Hyndman and Rogers 2010). Three earthquake types, namely shallow crustal earthquakes, deep in-slab earthquakes, and megathrust Cascadia interface earthquakes, contribute significantly to overall seismic hazard (Atkinson and Goda 2011). Since 1900, several destructive earthquakes occurred [Fig. 2(a)]: the 1918 and 1946 earthquakes in Vancouver Island; and the 1949, 1965, and 2001 (Nisqually) deep earthquakes in the U.S. state of Washington. Moreover, paleo-seismic data, such as onshore tsunami deposits and submarine turbidite deposits (Satake et al. 2003; Goldfinger et al. 2012), indicate that megathrust earthquakes had occurred repeatedly in the Cascadia subduction zone, involving the oceanic Juan de Fuca, Gorda, and Explorer plates moving against the continental North American plate. An example of typical ground motion for the three earthquake types is presented in Fig. 2(b). Because of different source and path characteristics of these earthquakes, amplitude, duration, and frequency content of typical ground motion for the three types differ.

The main objectives of this study are two-folds. The first aim is to demonstrate how recent advancements of the PBEE methodology affect the seismic risk assessment by focusing upon a 4-story nonductile reinforced concrete (RC) building located in Victoria as a case study (Tesfamariam and Goda 2015). The detailed seismic hazard characteristics attributable to three earthquake types (i.e., crustal, in-slab, and interface) are taken into account in developing seismic vulnerability models of the RC building. The second aim is to discuss how to improve seismic risk management capability by utilizing results from the advanced research. The new scientific knowledge and computational tools enable more accurate evaluations of disaster risk reduction alternatives (e.g., retrofitting, insurance, and risk transfer) via lifecycle cost-benefit analysis and catastrophe modeling (Goda and Hong 2006; Yoshikawa and Goda 2014). The novel aspects that are considered in the adopted PBEE method are

1. Record selection for subduction environments using extensive ground motion datasets (including the 2011 Tohoku earthquake records, which can be regarded as closest proxy for the Cascadia subduction events);
2. Consideration of main shock-aftershock (MS-AS) sequences as earthquake excitation; and

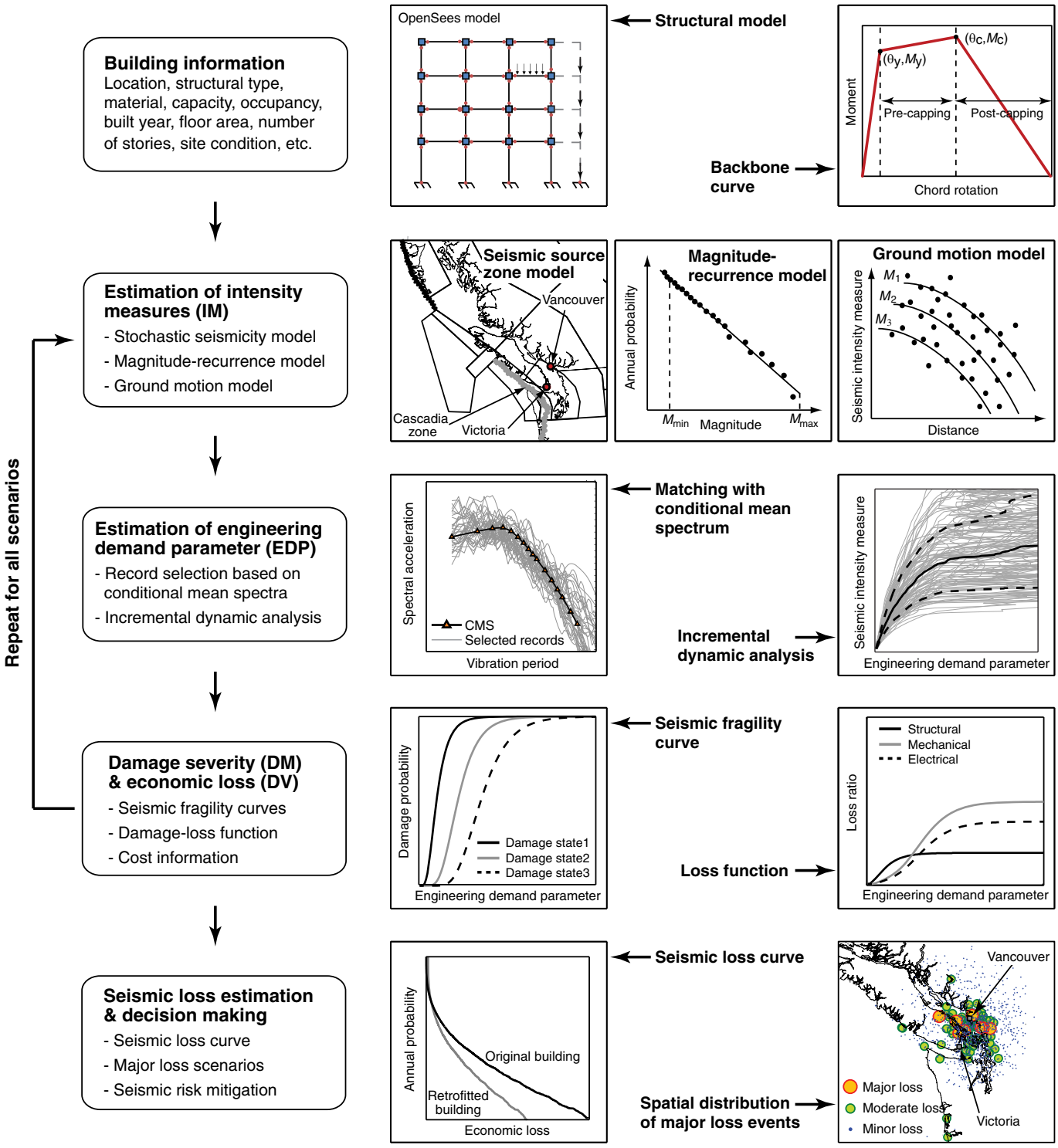

Fig. 3. Probabilistic seismic loss estimation framework

3. Multivariate seismic demand modeling for multicriteria seismic performance evaluation.

The paper is organized as follows. In the next section, the PBEE methodology is introduced and key model components are presented. Subsequently, results of the seismic risk assessment of the 4-story RC building are investigated by focusing upon the seismic loss impact attributable to different earthquake types, aftershock effects, and demolition-related loss generation. Finally, policy as well as strategic implications of the advanced PBEE assessment tools are discussed for earthquake risk reduction purposes.

Methodology

General Framework

A computational flow of the PBEE framework is illustrated in Fig. 3. The analytical procedure consists of seismic hazard analysis, structural analysis, and damage-loss analysis. Mathematically, the annual mean rate of exceeding a seismic performance metric $\nu(\mathrm{DV})$ (note: the consequence is represented by the decision variable, DV) can be expressed as follows:

$$\nu(\mathrm{DV}) = \iint G(\mathrm{DV}|\mathrm{EDP})|dG(\mathrm{EDP}|\mathrm{IM})||d\lambda(\mathrm{IM})| \qquad (1)$$

where $\lambda(\mathrm{IM})$ = mean annual rate of exceeding a given seismic intensity measure (IM) level and is obtained from probabilistic seismic hazard analysis (PSHA). The structural analysis develops a probabilistic relationship between IM and engineering demand parameter (EDP), which is denoted by the complementary cumulative probability distribution function $G(\mathrm{EDP}|\mathrm{IM})$. Typical EDP parameters include the maximum and residual interstory drift ratios (denoted by MaxISDR and ResISDR, respectively) and peak floor acceleration (PFA) for structural and nonstructural components. The damage-loss analysis relates EDP to seismic performance metric, DV (e.g., repair or reconstruction costs, downtime, and fatalities). Eq. (1) is formulated on the basis of so-called EDP-DV functions [i.e., $G(\mathrm{DV}|\mathrm{IM})$] by Ramirez and Miranda (2009). The details of the seismic loss model can be found in Tesfamariam and Goda (2015); thus, salient features only are mentioned in this study.

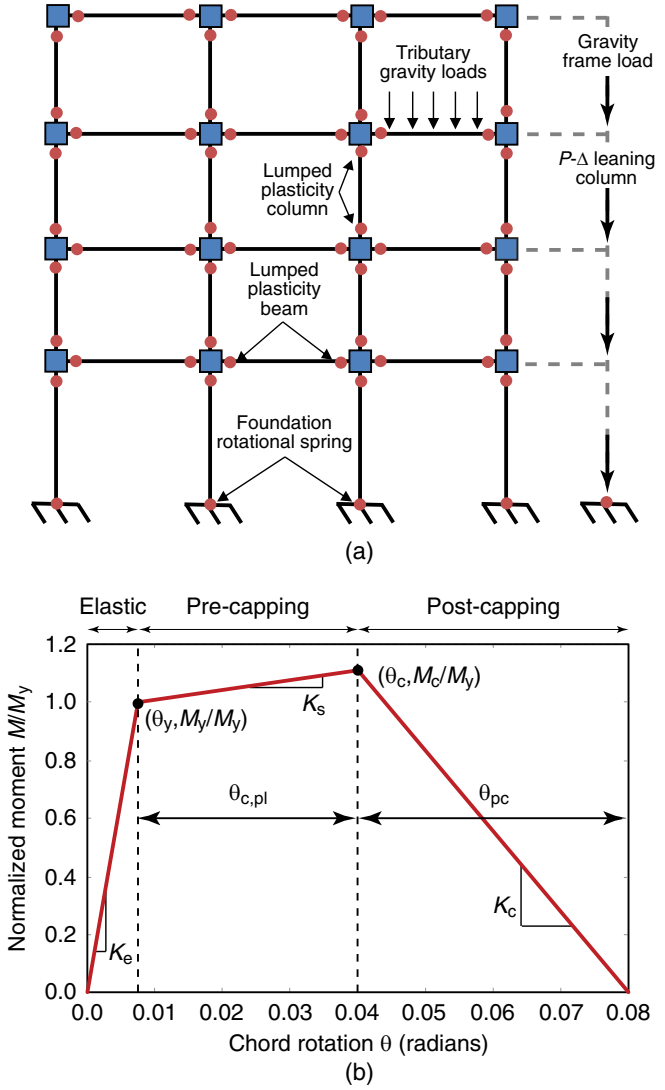

Fig. 4. (a) Nonlinear finite-element model of a 4-story non-ductile RC frame; (b) backbone curve for beam-column elements

Structural Model

A 4-story RC building is considered for the case study [Fig. 4(a)]. It has a floor area of 38.10 m by 53.34 m; columns are spaced at 7.62 m, and story heights are 4.57 m and 3.96 m at the ground floor and higher floor levels, respectively. The building model was developed by Liel and Deierlein (2008) according to the 1967 uniform building code (UBC) seismic provisions. More specifically, it was designed as a space frame, and all columns and beams were part of the lateral resisting system. Beam and column elements have the same amount of over-strength; each element is 15% stronger than the code-minimum design level. The design is governed by strength and stiffness requirements, as the 1967 UBC had few requirements for special seismic design or ductile detailing.

The nonductile RC structure is modeled in OpenSees using a lumped plasticity approach. The lumped plasticity element models used to simulate plastic hinges in beam-column elements utilize a nonlinear spring model [Fig. 4(b)]. This model is capable of capturing important modes of deterioration that lead to side-sway collapse of RC frames. Modal analysis of the finite-element model indicates that the first three modal periods are 1.92, 0.55, and 0.27 s, respectively.

Seismic Hazard and Ground Motion Selection

A case study site is focused upon Victoria, in which nonseismically-designed vulnerable RC frames exist and are still in use. There are three potential sources of damaging earthquakes in southwestern BC: shallow crustal earthquakes, deep in-slab earthquakes, and offshore megathrust interface earthquakes from the Cascadia subduction zone. The expected magnitude of the Cascadia events is in the range of M_w8 to M_w9; its mean recurrence period ranges from 500 to 600 years and the event occurred in the year of 1700. The regional seismicity in BC is represented by the seismic hazard model by Atkinson and Goda (2011), which is the updated version of the current national seismic hazard model in Canada (Adams and Atkinson 2003). Fig. 5 shows uniform hazard spectra (UHS) and seismic disaggregation results for Victoria (site class C) at the return period (T_R) of 2500 years. The spectral acceleration (SA) at 2.0 s is adopted as IM, noting that this spectral period is close to the fundamental vibration period of the 4-story nonductile RC frame. It is important to emphasize that a full range of uncertainty, as implemented in PSHA, is considered in the assessment. The seismic disaggregation results clearly identify the significant influence (50%) attributable to the Cascadia subduction events. This is an important consideration in selecting records for seismic performance evaluation of relatively flexible structures in Victoria.

The input ground motion records need to be selected carefully, because record scaling that is used for inelastic seismic demand modeling may induce bias in calculated structural responses. It is also important that selected time-histories have record characteristics (e.g., magnitude, duration, and spectral shape) that are similar to target seismic hazard in Victoria. For this purpose, a new ground motion record database has been compiled by including recent recordings from Japan, in particular, the 2011 M_w9 Tohoku earthquake records. The Tohoku dataset is relevant to the Cascadia event, because of anticipated similarity between these two megathrust subduction events, which is not present in ground motion data from other smaller earthquakes. The new ground motion database combines recordings from the next generation attenuation dataset and from three national and/or regional ground motion networks in Japan (i.e., K-NET, KiK-net, and SK-net). An innovative aspect of the database is that all time-history data are associated with actual MS-AS sequences. The combined database is comprised of 606 MS-AS record sequences; main shocks within

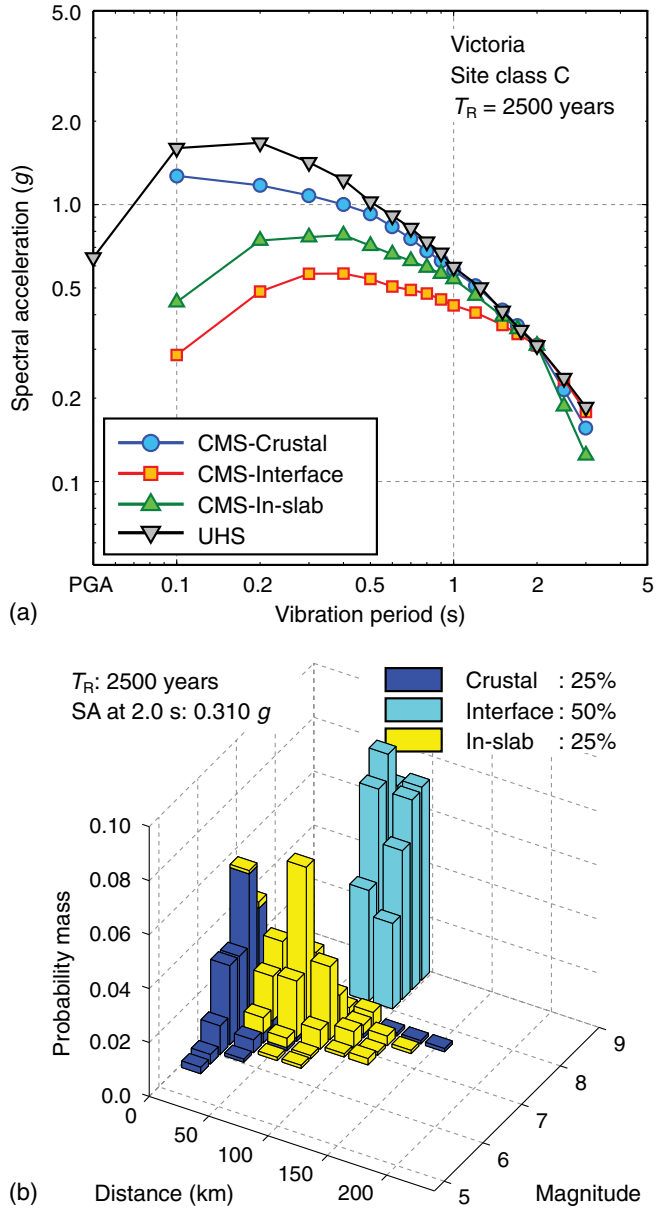

Fig. 5. (a) Uniform hazard spectra and conditional mean spectra for Victoria (site class C) at the return period of 2500 years; (b) seismic disaggregation for Victoria (site class C) at the return period of 2500 years

individual sequences are identified as events having the largest earthquake magnitude, and all main shock records have moment magnitudes greater than 5.9, rupture distances less than 300 km, and peak ground acceleration greater than 75 cm/s^2.

To avoid bias attributable to excessive record scaling in assessing seismic performance of a structure, a multiple conditional mean spectra (CMS) method is implemented by reflecting regional seismic hazard characteristics in BC (Goda and Atkinson 2011). The dominant earthquake scenarios that are necessary to define multiple target spectra (i.e., CMS) for three earthquake types (crustal, interface, and in-slab) are obtained from PSHA for Victoria [Fig. 5(a)]. Using the constructed ground motion database, 50 records (two horizontal components per record; i.e., 100 time-history data) are selected based on the multiple CMS method. The response spectra of the selected records match the target CMS over the vibration period range between 0.3 and 3.0 s. The number of records for each earthquake type, out of 50 records, is determined based on its relative contribution to seismic hazard using PSHA results. For the return period of 2500 years, the number of records for crustal, interface, and in-slab events is 13, 25, and 12, respectively. Representative MS-AS sequence data for the crustal, interface, and in-slab events are shown in Fig. 1(b).

Seismic Vulnerability and Damage Cost Model

Inelastic seismic demand prediction models are developed using incremental dynamic analysis (IDA) (Vamvatsikos and Cornell 2002). In IDA, a series of nonlinear dynamic analyses are conducted by scaling a set of input ground motions based on an adopted IM, and prediction equations of EDP at different IM levels are developed. IDA is carried out for the 4-story nonductile RC frame using the set of 50 MS-AS sequences. The spectral acceleration at 2.0 s (i.e., IM) ranges from 0.05 to 0.7g. For each nonlinear dynamic analysis, MaxISDR, ResISDR, and PFA at all four story levels are stored for postprocessing. Large MaxISDR and ResISDR values are observed at the ground floor level, when nonlinearity in the frame becomes severe, reflecting soft story collapse as a typical failure mode for this structure. In general, numerical instability is encountered when the interstory drift ratio of the frame exceeds 0.10. The first occurrence of such large deformation responses is treated as *collapse* (Vamvatsikos and Cornell 2002). A comparison of the collapse fragility curves for the three earthquake types is shown in Fig. 6(a). The results indicate that the collapse potential attributable to the interface events is greater than that attributable to the in-slab and crustal events. The IDA results for MaxISDR and ResISDR (ground floor) are shown in Figs. 6(b and c), respectively (the results for PFA are omitted for brevity; see Tesfamariam and Goda (2015) for the complete IDA results). To present the uncertainty of the IDA results succinctly, three percentile curves, i.e., median, 10th-percentile, and 90th-percentile, are included in the figure. The results shown in Figs. 6(b and c) suggest that the overall characteristics of the IDA curves for MaxISDR and ResISDR are different and the uncertainty of ResISDR is much greater than that of MaxISDR. Moreover, the earthquake event type has noticeable effects on the IDA results. For both MaxISDR and ResISDR, the median curves for interface events are severer than those for the crustal and in-slab events; i.e., for a given IM level (vertical axis), greater EDP values (horizontal axis) are attained. The increased seismic demand potential for the interface records is related to the rich long-period spectral content and the long-duration excitation. The latter makes noticeable influence, especially for ResISDR, because the structure tends to oscillate within an inelastic domain for a longer time. In short, physical features of ground motion records have influence on the seismic demand potential assessment.

At each IM level, multivariate seismic demand prediction models are developed for MaxISDR, ResISDR, and PFA (Tesfamariam and Goda 2015). Based on preliminary data analysis, MaxISDR and ResISDR are treated as dependent random variables, whereas PFA is independent of the other two. The marginal distribution types for MaxISDR and PFA are determined as the Frechet distribution, while the marginal distribution type for ResISDR is determined as the generalized Pareto distribution to capture the heavy right-tail characteristics. The dependence modeling of MaxISDR and ResISDR is then carried out using copulas (McNeil et al. 2005), which facilities separate modeling for marginal probability distribution and dependence function. The results indicate that the asymmetrical Gumbel copula is suitable for the majority of the examined cases. Accuracy of the joint probabilistic modeling of MaxISDR and ResISDR at the ground floor is confirmed

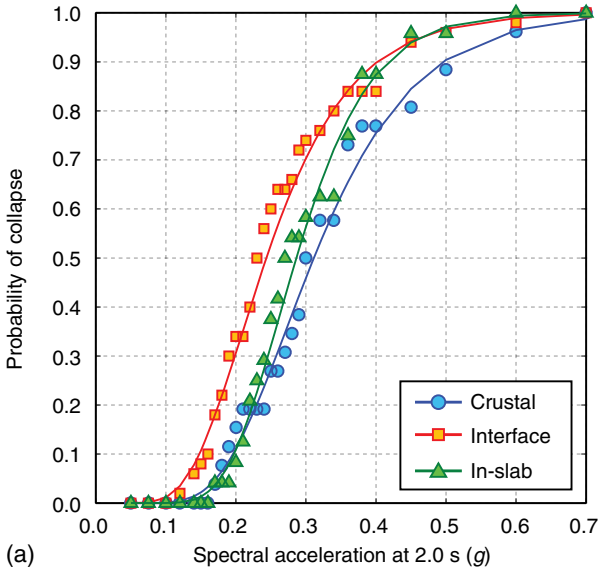

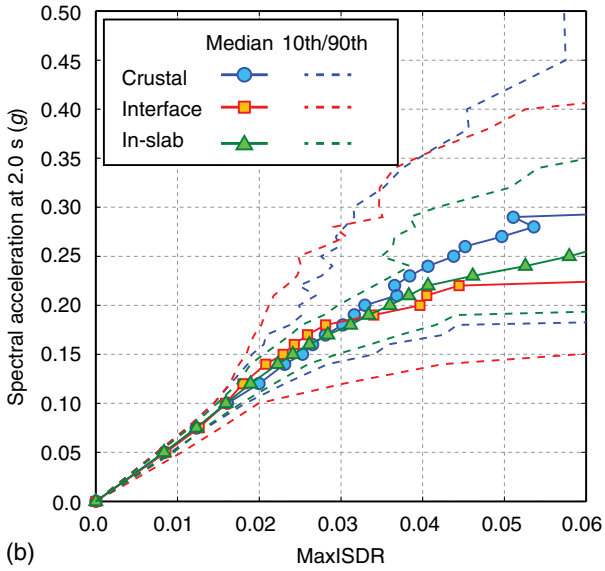

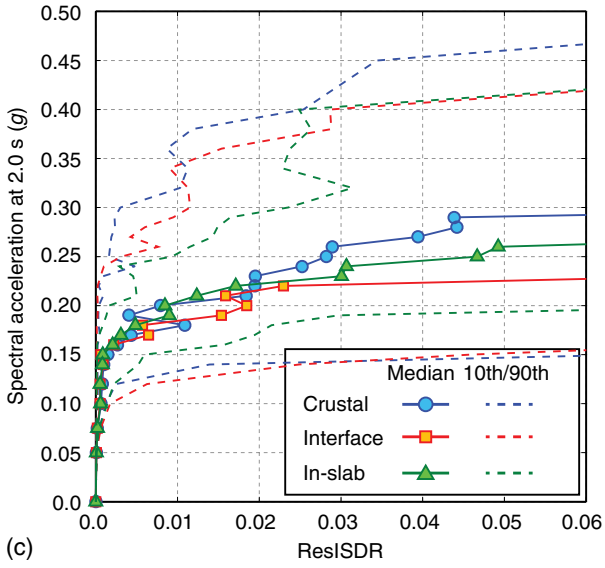

Fig. 6. Incremental dynamic analysis results for crustal, interface, and in-slab earthquakes by considering main shock–aftershock sequences: (a) collapse fragility curve; (b) maximum interstory drift ratio (MaxISDR); (c) residual interstory drift ratio (ResISDR)

visually by comparing simulated samples of these variables from the fitted probabilistic models with the IDA results at various seismic intensity levels (Goda and Tesfamariam 2015).

The damage-loss analysis relates EDP to DV through probabilistic loss models $G(\mathrm{DV}|\mathrm{EDP})$. In the developed seismic loss model, story-based damage-loss modeling methods by Ramirez and Miranda (2009) are adopted, where building components are grouped based on component and/or subcontractor type (e.g., concrete, metal, doors-windows-glass, finishes, electrical, or mechanical), story level, and damage sensitivity (i.e., drift-sensitive and acceleration-sensitive components). DV that is concerned in this study is direct economic loss (building repair and replacement costs); other seismic loss attributable to business interruption and relocation is not included. To account for the uncertainty related to damage cost estimation, EDP-DV functions are derived for 27 subcontractor-sensitivity story combinations (i.e., 9 subcontractor-sensitivity combinations; and ground, typical, or top). The distinction of the building story level stems from different building layout and use at different levels (which affect proportions of incurred seismic damage costs for different building components).

The seismic loss (L_T) for given EDP can be expressed as (Ramirez and Miranda 2009)

$$L_T = L_{\mathrm{NC}} + L_D + L_C \tag{2}$$

where L_{NC}, L_D, and L_C = seismic losses for noncollapse (NC) repairs, demolition (D), and collapse (C) cases, respectively. The three situations are disjoint and mutually exclusive. The numerical evaluation of L_T in the seismic risk assessment is facilitated as follows: (1) collapse probability is assessed using the collapse fragility curve based on MaxISDR [Fig. 6(a)]; if collapse is predicted, then $L_T = L_C$; (2) demolition of the structure is determined with regard to ResISDR in comparison with the (uncertain) limit state function for demolition; if demolition is predicted, then $L_T = L_D$; and (3) otherwise, L_{NC} is assessed by using EDP-DV functions for noncollapse cases. It is noted that L_{NC}, L_D, and L_C are random variables. The demolition and collapse (replacement) costs L_D and L_C can be simulated as lognormal variable. The median demolition and replacement costs can be estimated using mean unit-area construction and total floor area, and suitable values of damage cost variability can be assumed (typically, 0.6–0.7 in terms of coefficient of variation).

Seismic Loss Estimation of a Nonductile RC Frame in Victoria

Seismic Loss Estimation Procedure

This section presents seismic loss estimation results of the 4-story nonductile RC frame located in Victoria. The assessment integrates regional seismic hazard information and seismic vulnerability information of the structure. The effects attributable to major aftershocks are included as part of probabilistic inelastic seismic demand models. The computation is based on Monte Carlo simulation involving the following calculation steps (Fig. 3):

1. A synthetic earthquake catalog is generated using a regional seismic hazard model by Atkinson and Goda (2011). Areal and fault sources, together with their occurrence rates and magnitude-recurrence relationships, are employed to generate occurrence time, location (latitude, longitude, and depth), and moment magnitude of individual events. In addition, finite-fault planes are generated for calculating rupture distance accurately. All relevant uncertainty is taken into account (e.g., epistemic uncertainty related to alternative hypotheses for the Cascadia

subduction events). The simulation duration is set to 5 million years. The generated catalog contains approximately 2.1 million events above M_w5.

2. For each event, a value of IM (i.e., spectral acceleration at 2.0 s) is generated using a ground motion model. The ground motion model is selected from a set of applicable models that are adopted by Atkinson and Goda (2011), depending on earthquake type.
3. Given a value of IM, collapse probability is evaluated based on the IDA results [Fig. 6(a)]. When the occurrence of collapse is predicted, the collapse cost is generated from the lognormal distribution based on damage cost information. Proceed to Step 7.
4. Samples of EDP variables (i.e., MaxISDR, ResISDR, and PFA at the ground floor level) are generated using the multivariate inelastic seismic demand models (i.e., suitable probability distribution types and copula functions). The EDP responses at the higher floor levels are obtained using the response shape functions.
5. For a given value of ResISDR, demolition probability is evaluated. When the occurrence of demolition is predicted, the demolition cost is calculated in a similar manner as the collapse cost. Proceed to Step 7.
6. For cases where neither collapse nor demolition is predicted, noncollapse seismic loss is calculated using evaluated EDP values at different floor levels and contractor-based EDP-DV functions. The uncertainty and correlation of the EDP-DV functions are taken into consideration. Proceed to Step 7.
7. Repeat Steps 2–6 for all events contained in the synthetic catalog.
8. The estimated seismic loss is analyzed statistically to develop an annual seismic loss curve. The information on occurrence time in the synthetic earthquake catalog is used to convert scenario-based loss results to those on an annual basis.

In the developed model, additional features are implemented to enhance the capability of the seismic loss estimation tool. It is related to additional uncertainty for collapse fragility, noncollapse vulnerability models, and EDP-DV functions. Liel and Deierlein (2008) conducted rigorous assessment of epistemic uncertainty related to collapse fragility and suggested that logarithmic standard deviation obtained from the IDA results directly may be underestimated. They indicated that the logarithmic standard deviation accounting for epistemic uncertainty is approximately 0.5 (note: logarithmic standard deviation for aleatory uncertainty is approximately 0.4). Conversely, Jayaram et al. (2012) developed quantitative seismic vulnerability models for tall buildings in California by following the PBEE methodology. They emphasized that epistemic uncertainty related to noncollapse vulnerability should be included as the IDA results only do not capture a whole range of uncertainty. Based on the literature, they suggested that the additional logarithmic standard deviation for noncollapse vulnerability is approximately 0.25. Furthermore, Jayaram et al. (2012) discussed that uncertainty of seismic loss may be still underestimated. The previously-mentioned three types of uncertainty are incorporated in the model. The additional logarithmic standard deviation for collapse is combined with that estimated from the IDA results in Step (3). For the epistemic uncertainty related to EDP generation for noncollapse vulnerability and seismic loss estimation, additional uncertain factors, which are lognormally distributed, are generated and are multiplied by the simulated EDP and total seismic loss.

Seismic Loss Estimation Results

Using the previously-mentioned PBEE-based model, seismic loss estimation of the 4-story nonductile RC building is carried out. A series of sensitivity analyses are conducted by considering different model components/settings. The results are discussed in Tesfamariam and Goda (2015) and are not repeated herein. Rather, in this study, comparisons of the seismic loss estimation results for different earthquake types (i.e., crustal, interface, and in-slab) and for extended and conventional PBEE procedures are focused upon. In the extended procedure, aftershock effects and demolition-based loss generation are taken into account, in comparison with the conventional procedure. The aim of these comparisons is to highlight the impact of the improved analysis tools on the seismic risk assessment quantitatively.

Fig. 7 compares annual seismic loss curves for all, crustal, interface, and in-slab earthquakes. The seismic loss (horizontal axis) is normalized with respect to the total replacement cost of the 4-story RC frame ($12.6 million). The vertical axis for Fig. 7(a) corresponds to the annual exceedance probability, whereas that for

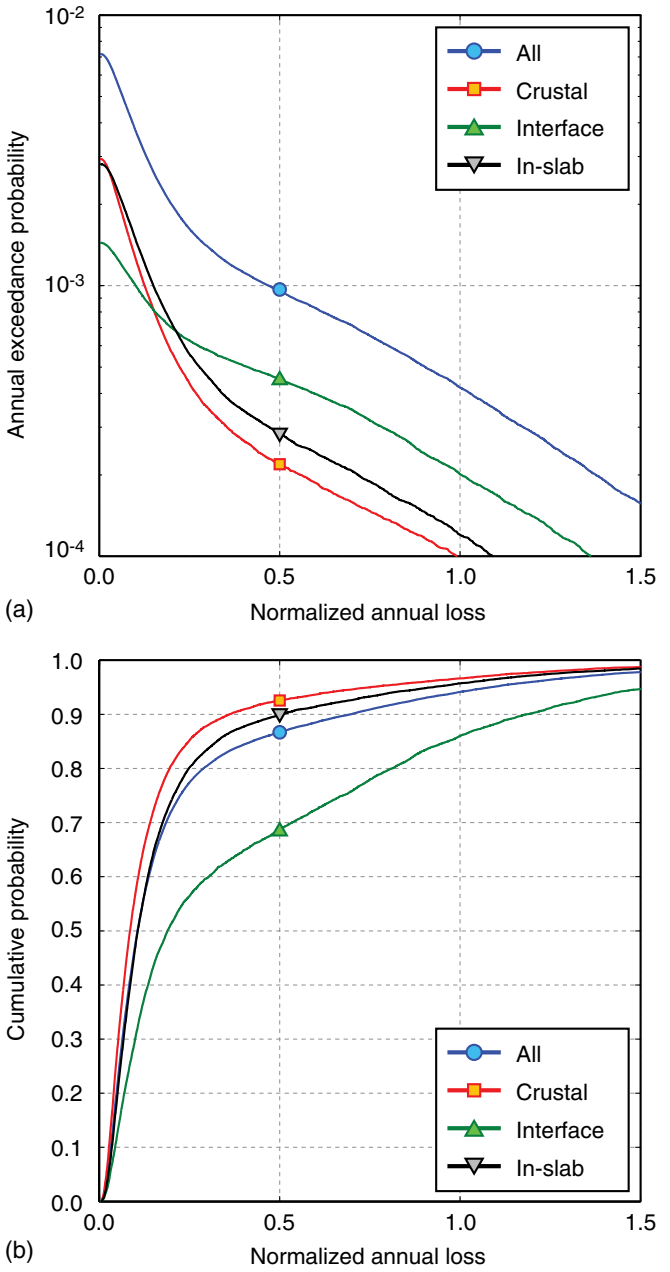

Fig. 7. Normalized annual loss curves for all, crustal, interface and in-slab earthquakes: (a) unconditional cases; (b) conditional cases

Table 1. Summary of Seismic Loss Estimation Results for All and Three Earthquake Types by Considering Two Cases: MS-AS Demand with Demolition Loss Generation and MS-Only Demand without Demolition Loss Generation

	MS-AS demand with demolition				MS-only demand without demolition			
Variable	All	Crustal	Interface	In-slab	All	Crustal	Interface	In-slab
Annual occurrence rate	0.0072	0.0029	0.0014	0.0028	0.0072	0.0029	0.0014	0.0028
Mean annual loss	0.00177	0.00052	0.00064	0.00061	0.00162	0.00048	0.00059	0.00055
SD annual loss	0.0387	0.0192	0.0261	0.0213	0.0361	0.0175	0.0247	0.0197
Conditional mean loss	0.2458	0.1779	0.4409	0.2170	0.2244	0.1612	0.4075	0.1969
Conditional SD loss	0.3847	0.3052	0.5282	0.3365	0.3613	0.2801	0.5062	0.3143
0.999-fractile annual loss	0.4696	0.1258	0.1012	0.1500	0.3850	0.1183	0.0956	0.1409
0.9999-fractile annual loss	1.7042	0.9916	1.3625	1.0921	1.6667	0.8325	1.3080	0.9698

Note: SD = standard deviation.

Fig. 7(b) corresponds to the conditional cumulative probability for seismic loss. In other words, Fig. 7(a) shows the unconditional seismic loss curves, taking into account the occurrence of damaging earthquakes, whereas Fig. 7(b) shows the conditional seismic loss functions, representing the seismic loss given the occurrence of a major earthquake. Both seismic loss results are useful for seismic risk management. Based on the unconditional results [Fig. 7(a)], various seismic risk metrics, such as annual expected loss (AEL) and value at risk (VaR) (Yoshikawa and Goda 2014), can be evaluated. Table 1 summarizes several key risk metrics that are derived from the seismic loss curves shown in Fig. 7. These metrics include: annual occurrence probability, mean annual loss (= AEL), standard deviation of annual loss, conditional mean loss, conditional standard deviation of seismic loss, 0.999-fractile annual loss, and 0.9999-fractile annual loss. The latter two are referred to as VaR at 0.999 and 0.9999 fractile levels.

Fig. 7(a) indicates that all three earthquake types contribute to the overall seismic loss for the 4-story RC building. The relative contributions depend on the annual probability level, because the underlying dominant earthquakes gradually change with the annual probability level [note: variable dominant event types can be investigated by generating seismic disaggregation results at different probability levels as shown in Fig. 5(b)]. At the annual probability levels between 10^{-2} and 10^{-3}, crustal and in-slab events are the main causative earthquakes for seismic loss because the frequency of moderate crustal and in-slab events near Victoria is greater than that of the Cascadia events, although the magnitudes of crustal and in-slab events ($M_w 6.5 - M_w 7.5$) are smaller than those attributable to the Cascadia events ($M_w 8.5$ to $M_w 9.0$). When the rare probability levels between 10^{-3} and 10^{-4} are focused upon, the potential impact attributable to the Cascadia megathrust events becomes dominant. This is because at the small annual probability levels, the occurrence of the Cascadia event (whose annual occurrence probability is set to a range between $1/600$ and $1/500$ in the seismic hazard model) is considered as likely, and given occurrence the impact attributable to the Cascadia interface events is greater than those attributable to other events. This is indeed shown in Fig. 7(b) (i.e., conditional cumulative probability distribution functions of seismic loss for crustal, interface, and in-slab events). This difference is attributable to different physical characteristics of the crustal, interface, and in-slab events (combinations of magnitude and distance) and their influence on structural responses. It is noteworthy that the consideration of the Cascadia subduction events in PSHA and regional seismic loss studies is relatively recent. In the 1990's, the evidence for the Cascadia subduction zone had emerged in the scientific literature; nevertheless, the potential influence attributable to the Cascadia events was not taken into account before the 2005 version of the national seismic hazard model for Canada (Adams and Atkinson 2003). In the last decade, the potential risks attributable to the Cascadia subduction events are widely recognized in the scientific and engineering communities and various improvements have been suggested (Atkinson and Goda 2011; Tesfamariam and Goda 2015). The current knowledge and understanding of the Cascadia subduction events are likely to be further updated in the future. Using the advanced seismic loss estimation tools, the value of new information and improved knowledge can be assessed and appreciated. For instance, as shown in Fig. 7(a), inclusion of the Cascadia subduction events in the seismic loss assessment changes the seismic loss curves significantly (note: this corresponds to pre-2005 versus post-2005 situations in Canada). The extent of the underestimation of the seismic risks is greater for flexible structures than stiff structures (Koduru and Haukaas 2010). This has important implications on the seismic design provisions for high-rise and tall buildings.

The refined PBEE-based seismic loss model has incorporated several key seismic vulnerability model components such that aftershock-related seismic loss as well as demolition-related economic loss is taken into account (Tesfamariam and Goda 2015). To examine the impact of this inclusion, the seismic risk metrics are calculated for the case with main shocks only and without demolition-related loss generation, and are also included in Table 1. Comparison of the risk metrics for the two cases indicates that the consideration of aftershock effects and demolition-related loss increases the risk metrics by approximately 5–12%. For the 4-story RC structure, the effects attributable to aftershocks are approximately 0–5%, while the effects attributable to demolition are approximately 5–10%. These numbers are likely to differ for different types of structures (e.g., resisting mechanism, material, height, and applied seismic design provision). Typically, the aftershock effects tend to be greater for stiff structures because the dominant aftershocks have richer spectral content in the short vibration period range. Moreover, values of ResISDR depend on the earthquake event type [Fig. 6(c)]. Therefore, consideration of demolition affects the relative seismic loss contributions attributable to different earthquake scenarios. The advanced seismic loss estimation tools promote the deeper understanding of the main causes of seismic loss generation and their complex interaction. These tools are essential for evaluating the effectiveness of the earthquake risk reduction measures.

Policy and Risk Management Implications

Risk management is a process of weighting alternatives and selecting the most appropriate action by integrating the results of risk assessment with engineering data as well as social/economic/political factors. The damage and loss observed from recent earthquakes highlight the need for an improved seismic risk analysis tool

to prioritize resources in assessing and retrofitting deficient buildings. In assessing seismic risk quantitatively, uncertainty is prevalent in spatiotemporal characterization of earthquake occurrence, ground motion prediction, building stock exposure, seismic fragility of structures, and loss generation mechanism. In particular, modeling and treatment of epistemic uncertainty are critically important. The PBEE-based seismic risk assessment framework serves as a useful decision support tool for earthquake risk mitigation and facilitates the prioritization of available options from the structural reliability and economic viewpoints.

The current framework for seismic risk analysis addresses earthquake-induced hazards, vulnerability of structural/nonstructural components, and consequences attributable to damage. As highlighted in the illustrative application of the PBEE, accurate assessment of potential hazards, building information, and dependency among different DVs can furnish valuable data for risk assessment and informed decision-making. For effective disaster risk mitigation, separate seismic vulnerability models for different earthquake types are useful, and different risk mitigation measures may be necessary for different types of events (or hazards). For instance, installing dampers may be effective in suppressing vibrations in structures that are susceptible to long-duration and long-period motion attributable to large subduction events (Takewaki et al. 2011). As such, the loss estimation results should explicitly account for different earthquake types and consider extension of loss modeling components for aftershocks and demolition. More tailored risk management is now possible taking advantages of improved methods.

The risk framework developed for a single building can be extended to a portfolio of buildings and infrastructure, distributed over different scales (e.g., city blocks and neighborhood communities, municipalities, and regions). For the case of BC, the type of earthquakes considered for seismic risk management, e.g., crustal scenarios versus interface scenarios, has major influence on the disaster preparedness planning. This is because the Cascadia earthquakes affect much wider areas (entire region), disturbing numerous urban districts and residential communities simultaneously, in comparison with moderate crustal earthquakes, potentially causing destructive damage and loss to local areas. In such cases, emergency management teams should be able to respond to both types of catastrophes. More broadly, these have important implications on the preparedness, evacuation, early warning, and risk prioritization.

Another important issue related to post-disaster policy and management is the potential risks attributable to large aftershocks. The likelihood of major aftershocks decay with time after the occurrence of a main shock (e.g., according to the modified Omori law) and, thus, evacuation orders may be canceled when the residual risks attributable to ongoing aftershock sequences are judged to be manageable. As the large subduction events trigger numerous aftershocks over a prolonged period (e.g., 2004 Sumatra earthquake and 2011 Tohoku earthquake; Shcherbakov et al. 2013), time to reach such decisions by emergency managers may vary significantly. Potential risks and rationales for their decisions need to be communicated effectively with evacuees who face anxiety and inconvenience. The refined PBEE-based method can provide an objective decision basis by evaluating time-varying life safety risks in the aftershock environment (Yeo and Cornell 2009). Moreover, there is considerable uncertainty related to the spatial evolution of aftershock sequences. A recent notable example that posed major challenges is the 2010–2011 Christchurch sequences (Shcherbakov et al. 2012); the sequences initiated by the 2010 M_w7.1 Darfield earthquake had evolved towards the city of Christchurch and had triggered destructive earthquakes near the downtown Christchurch. The latter aspect has not yet been accounted for in the current PBEE methodology. The incorporation of emerging scientific information and theory in developing new risk analysis tools is essential and will enhance the utility of the advanced seismic risk assessment methodology for policy and risk management purposes.

Lastly, the PBEE-based risk assessment can be extended to other natural disasters, such as tsunamis. The probabilistic tsunami risk analysis can take into account uncertain tsunami hazard scenarios and tsunami vulnerability of buildings to assess potential impact of future destructive tsunamis (Goda et al. 2015b). The outputs from probabilistic tsunami hazard and risk analyses include stochastic inundation maps, stochastic tsunami damage probability maps, and tsunami risk-loss curves. These are particularly useful for risk communication, evacuation and emergency response, and risk management. Moreover, consideration of common earthquake source rupture processes for strong motion and tsunami facilitates a novel multihazard assessment method for cascading shaking-tsunami sequences (Goda et al. 2015a). The new assessment tools improve current practices of preparing earthquake and tsunami hazard maps, which are prepared separately and are based on different methods, data, assumptions, and scenarios. Importantly, they promote consistent ground shaking and tsunami hazard/risk maps and assessments that correspond to the same set of earthquake scenarios and, thus, can be used together in disaster risk management.

Conclusions

Seismic risk analysis and management are of paramount importance to mitigate any future seismic induced damage. The life safety objectives in developed countries have been met through effective building design codification and its enforcement. The unacceptably high economic loss, however, has provided the motivation for the PBEE methodology that aims at reducing the economic/financial consequences of earthquake disasters, in addition to the life safety requirement. In this paper, through a case study, effects of earthquake types and improved model components on the loss assessment are quantified. The results clearly show that the earthquake type has different energy content, amplitude, and duration and, thus, may affect different buildings and infrastructure significantly. Furthermore, the different earthquakes have different impacts in terms of damage concentration and spatial extent of the affected areas. To extend the capability in dealing with emerging hazards and risks, the risk analysis tools should evolve dynamically. Most importantly, risk mitigation policies need to be developed in light of current knowledge substantiated by advanced risk analysis methods and tools.

Acknowledgments

The authors acknowledge Abbie Liel for generously sharing her OpenSees model for the noncode conforming RC building. Ground motion data for Japanese earthquakes and worldwide crustal earthquakes were obtained from the K-NET/KiK-net/SK-net databases at http://www.kyoshin.bosai.go.jp/ and http://www.sknet.eri.u-tokyo.ac.jp/, and the PEER-NGA database at http://peer.berkeley.edu/nga/index.html, respectively. This work was supported by the Engineering and Physical Sciences Research Council (EP/M001067/1) to the first author, and the Natural Sciences and Engineering Research Council of Canada (NSERC) Discovery Grants Program (RGPIN-2014-05013) to the second author.

References

Adams, J., and Atkinson, G. M. (2003). "Development of seismic hazard maps for the proposed 2005 edition of the National Building Code of Canada." *Can. J. Civ. Eng.*, 30(2), 255–271.

AIR Worldwide. (2013). "Study of impact and the insurance and economic cost of a major earthquake in British Columbia and Ontario/Québec." *Prepared for Insurance Bureau of Canada*, Toronto, Canada.

Atkinson, G. M., and Goda, K. (2011). "Effects of seismicity models and new ground motion prediction equations on seismic hazard assessment for four Canadian cities." *Bull. Seismol. Soc. Am.*, 101(1), 176–189.

Cornell, C. A., Jalayer, F., Hamburger, R. O., and Foutch, D. A. (2002). "Probabilistic basis for 2000 SAC Federal Emergency Management Agency steel moment frame guidelines." *J. Struct. Eng.*, 10.1061/(ASCE)0733-9445(2002)128:4(526), 526–533.

Goda, K., and Atkinson, G. M. (2011). "Seismic performance of wood-frame houses in south-western British Columbia." *Earthquake Eng. Struct. Dyn.*, 40(8), 903–924.

Goda, K., De Risi, R., and Rossetto, T. (2015a). "Coupled simulation of ground shaking and tsunami for mega-thrust subduction earthquakes." *Proc., 12th Int. Conf. on Applications of Statistics and Probability in Civil Engineering*, Vancouver, Canada.

Goda, K., and Hong, H. P. (2006). "Optimal seismic design for limited planning time horizon with detailed seismic hazard information." *Struct. Saf.*, 28(3), 247–260.

Goda, K., Li, S., Mori, N., and Yasuda, T. (2015b). "Probabilistic tsunami damage assessment considering stochastic source models: Application to the 2011 Tohoku earthquake." *Coastal Eng.*, 57(3), 1550015.

Goda, K., and Tesfamariam, S. (2015). "Multi-variate seismic demand modelling using copulas: Application to non-ductile reinforced concrete frame in Victoria, Canada." *Struct. Saf.*, 56(1), 39–51.

Goldfinger, C., et al. (2012). *Turbidite event history—Methods and implications for Holocene paleoseismicity of the Cascadia subduction zone*, U.S. Geological Survey, 170.

Goulet, C. A., et al. (2007). "Evaluation of the seismic performance of a code-conforming reinforced-concrete frame building—From seismic hazard to collapse safety and economic losses." *Earthquake Eng. Struct. Dyn.*, 36(13), 1973–1997.

Hyndman, R. D., and Rogers, G. C. (2010). "Great earthquakes on Canada's west coast: A review." *Can. J. Earth Sci.*, 47(5), 801–820.

Jayaram, N., Shome, N., and Rahnama, M. (2012). "Development of earthquake vulnerability functions for tall buildings." *Earthquake Eng. Struct. Dyn.*, 41(11), 1495–1514.

Koduru, S. D., and Haukaas, T. (2010). "Probabilistic seismic loss assessment of a Vancouver high-rise building." *J. Struct. Eng.*, 10.1061/(ASCE)ST.1943-541X.0000099, 235–245.

Li, Q., and Ellingwood, B. R. (2007). "Performance evaluation and damage assessment of steel frame buildings under main shock-aftershock earthquake sequences." *Earthquake Eng. Struct. Dyn.*, 36(3), 405–427.

Liel, A. B., and Deierlein, G. G. (2008). "Assessing the collapse risk of California's existing reinforced concrete frame structures: Metrics for seismic safety decisions." *John A. Blume Earthquake Engineering Center Rep. No. 166*, Dept. of Civil and Environmental Engineering, Stanford Univ., Stanford, CA.

McNeil, A. J., Frey, R., and Embrechts, P. (2005). *Quantitative risk management: Concepts, techniques and tools*, Princeton University Press, Princeton, NJ.

Mitchell, D., et al. (2010). "Evolution of seismic design provisions in the National Building Code of Canada." *Can. J. Civ. Eng.*, 37(9), 1157–1170.

Onur, T., Ventura, C. E., and Finn, W. D. L. (2005). "Regional seismic risk in British Columbia—Damage and loss distribution in Victoria and Vancouver." *Can. J. Civ. Eng.*, 32(2), 361–371.

Raghunandan, M., Liel, A. B., and Luco, N. (2015). "Collapse risk of buildings in the Pacific northwest region due to subduction earthquakes." *Earthquake Spectra*, 31(4), 2087–2115.

Ramirez, C. M., and Miranda, E. (2009). "Building-specific loss estimation methods & tools for simplified performance-based earthquake engineering." *John A. Blume Earthquake Engineering Center Rep. No. 171*, Dept. of Civil and Environmental Engineering, Stanford Univ., Stanford, CA.

Ruiz-García, J. (2012). "Mainshock-aftershock ground motion features and their influence in building's seismic response." *J. Earthquake Eng.*, 16(5), 719–737.

Satake, K., Wang, K., and Atwater, B. F. (2003). "Fault slip and seismic moment of the 1700 Cascadia earthquake inferred from Japanese tsunami descriptions." *J. Geophys. Res. Solid Earth*, 108(B11), 2535.

Shcherbakov, R., Goda, K., Ivanian, A., and Atkinson, G. M. (2013). "Aftershock statistics of major subduction earthquakes." *Bull. Seismol. Soc. Am.*, 103(6), 3222–3234.

Shcherbakov, R., Nguyen, M., and Quigley, M. (2012). "Statistical analysis of the 2010 M_W 7.1 Darfield earthquake aftershock sequence." *N. Z. J. Geol. Geophys.*, 55(3), 305–311.

Takewaki, I., Murakami, S., Fujita, K., Yoshitomi, S., and Tsuji, M. (2011). "The 2011 off the Pacific coast of Tohoku earthquake and response of high-rise buildings under long-period ground motions." *Soil Dyn. Earthquake Eng.*, 31(11), 1511–1528.

Tesfamariam, S., and Goda, K. (2015). "Loss estimation for non-ductile reinforced concrete building in Victoria, British Columbia, Canada: Effects of mega-thrust M_w9-class subduction earthquakes and aftershocks." *Earthquake Eng. Struct. Dyn.*, 44(13), 2303–2320.

Tesfamariam, S., Goda, K., and Mondal, G. (2015). "Seismic vulnerability of RC frame with unreinforced masonry infill due to mainshock-aftershock earthquake sequences." *Earthquake Spectra*, 31(3), 1427–1449.

Vamvatsikos, D., and Cornell, C. A. (2002). "Incremental dynamic analysis." *Earthquake Eng. Struct. Dyn.*, 31(3), 491–514.

Wen, Y. K., and Ellingwood, B. R. (2005). "The role of fragility assessment in consequence-based engineering." *Earthquake Spectra*, 21(3), 861–877.

Yeo, G. L., and Cornell, C. A. (2009). "Equivalent constant rates for post-quake seismic decision making." *Struct. Saf.*, 31(5), 443–447.

Yoshikawa, H., and Goda, K. (2014). "Financial seismic risk analysis of building portfolios." *Nat. Hazards Rev.*, 10.1061/(ASCE)NH.1527-6996.0000129, 112–120.